

Characterizing and solving imaging challenges in thick resists for wafer and panel based lithography applications

James E. Webb, Roger McCleary
Rudolph Technologies, Inc.
16 Jonspin Rd
Wilmington, MA 01880
Ph: 978-253-6204; Fax: 978-658-6349
Email: james.webb@rudolphtech.com

Abstract

Increasing volume using larger substrates with decreasing process margins continues to create new challenges for advanced packaging applications. Key step and repeat camera technology continues evolving for the mass production of microstructures used for 2.5D and 3D technologies. Printing dense arrays of smaller features with high aspect ratios requires higher sidewall angles in thick photoresists and polyimides. To help solve these imaging challenges we have leveraged resist modeling software and guided the adjustment of optical parameters needed for better performance. Higher contrast films have also been evaluated to help achieve the improvements in performance needed. Resist models that can include the effects of flare have been critical to understand the requirement for printing in thick negative resists and has aided in printing features on varying topography and film thicknesses. Special chucks help improve the flatness of warped wafers and real-time auto-focusing provides good image fidelity. Printing microstructures over larger formats with higher throughput has been accomplished using large magnification adjustment for improving overlay and validated by characterizing image placement errors over large substrates. Examples of resist models that are created using resist parameters and optimized using SEM images of printed features are compared. Extrapolations of the resist models have shown that guide improvements can be achieved by varying optical parameters. SEM images confirm that the modeled result of the optimal solution was achieved. Reduction in large substrate overlay error was achieved after the stage corrections were applied. Examples show that topographical errors of warped wafers can be reduced and how real-time auto-focusing for each exposure minimizes focus errors.

Key words

Projection lithography, stepper, thick films, redistribution layer (RDL), via, photoresist modeling

Introduction

Many of the early photoresists developed for advanced packaging had low contrast compared to new photoresists available for use today for the most challenging requirements of advanced packaging. Higher numerical aperture projection lenses were utilized to print structures in thick photoresists with steep sidewall angles. Higher numerical aperture lenses print a smaller image field with less depth of focus and do not compensate for magnification adjustments that may be required to compensate for die shift. These attributes severely limit corrections required on

larger panel type substrates being introduced for large scale production of devices with lower cost of ownership.

Printing multiple layers in thick photoresists and polyimides is a requirement for many advanced packaging applications. The sidewall angle (SWA) required for imaging in a given photoresist thickness layer is determined by the contrast (γ) of the photoresist at the required aspect ratio (AR) and the imaging fidelity that is best described by the normalized log slope (NLS) of the image [1]. Numerical aperture of the lens, wavelengths used, type of illumination, partial coherence, and lens aberrations including defocus all

control the log slope of the image. The NILS is determined by multiplying the critical dimension (CD) with the image log slope (ILS). Background intensity or flare also impact the performance. Their relationship is described by the following equations (1), (2):

$$\text{NILS} = \text{CD} \times \text{ILS} \quad (1)$$

and

$$\text{SWA} = \tan^{-1}(\gamma_{\text{AR}} \times \text{NILS}) \quad (2)$$

Significant advances in photoresist technology are making it possible to achieve the imaging performance needed in thick photoresists (PR) and polyimides (PI) while utilizing lower numerical apertures. Lower numerical aperture provides greater depth of focus needed to image a larger field size on larger substrates with higher topographical variations. The higher the photoresist contrast is the lower the NILS value needed to print the same sidewall angle in photoresist.

Fig. 1 is an example of SEM cross sections of 2 μm lines and spaces (RDL) printed in a 10 μm film thickness of a chemically amplified photoresist on Si at 540 mJ dosage. Using ghi-lines at NA 0.1, a focal depth of 28 μm with sidewall angle (SWA) greater than 88.8° is achieved. This is only attainable with photoresist contrast $\gamma > 20$.

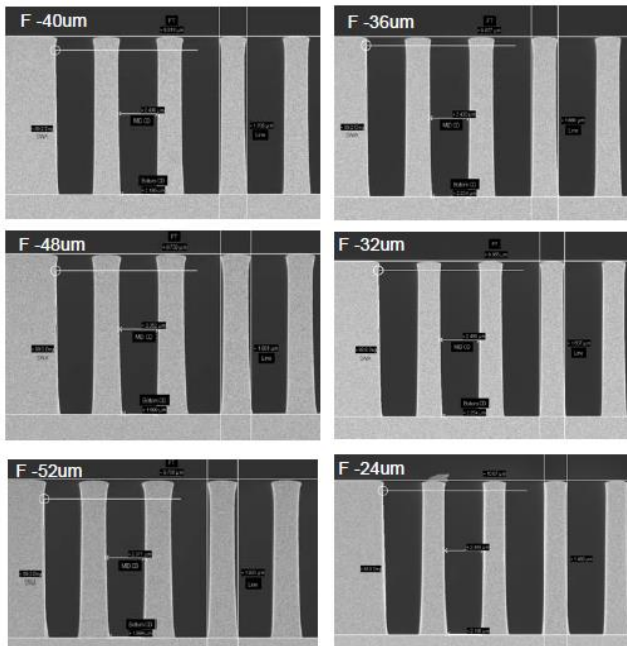


Fig. 1: SEM measured cross section measurements of 2 μm l/s in 10 μm FT chemically amplified photoresist

GenISys Lab resist modeling software uses fitting algorithms to determine the parameters used for image analysis based on the measured gamma curves in Fig. 2 [2]. Fine adjustments are made to match the model to the measured SEM cross sections.

- Resist and exposure characteristics needed for modeling

- Resist contrast γ
- Dill C
- n and k parameters
 - Unbleached and bleached
 - Wavelength weighting
 - Development time
- Terms used for calibration
 - Rate of development
 - Slope
 - M_{th}
 - Diffusion length
 - Surface inhibition

Resist contrast data and calibration

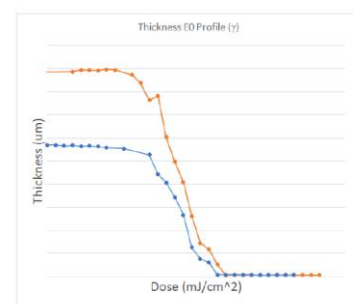


Fig. 2: Gamma curves for two different thicknesses of the same positive photoresist are shown

A side profile of the SEM measured CD is compared to the photoresist model shown in Fig. 3.

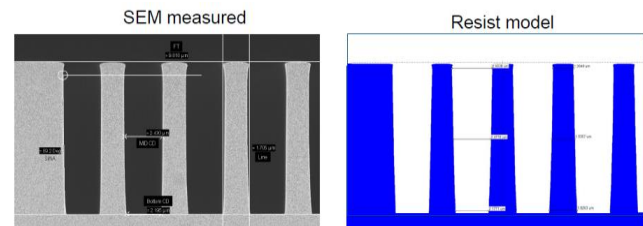


Fig. 3: Modeled and measured photoresist images are compared

Fig. 4 compares the photoresist model through focus to measured CDs through focus at different locations from the bottom to top of the film thickness. Once validated this model can be used to extrapolate performance using different optical and photoresist process parameters.

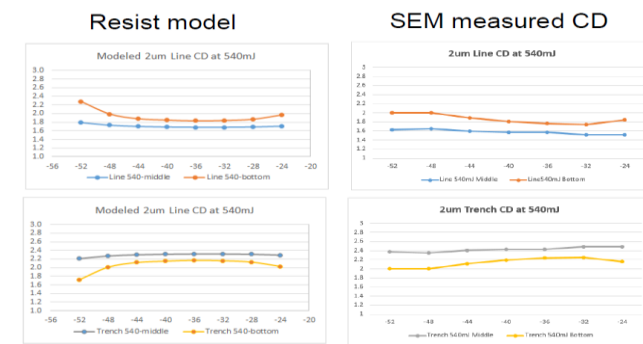


Fig. 4: Photoresist model compared to measured CDs through focus

Fig. 5 shows improvements in imaging performance obtained by implementing modifications determined by the photoresist model. In this study the sidewall angle in the thick photoresist and CD dimension of the thin photoresist are optimized.

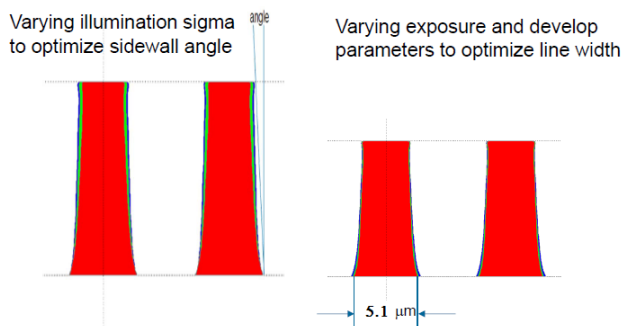


Fig. 5: Examples of photoresist models used to guide optimal performance

SEM images in Fig. 6 confirm that the modeled result of the optimal solution is achieved. Lab metrology can compute the CD variation at both the top and bottom of the photoresist as shown in Fig. 7.

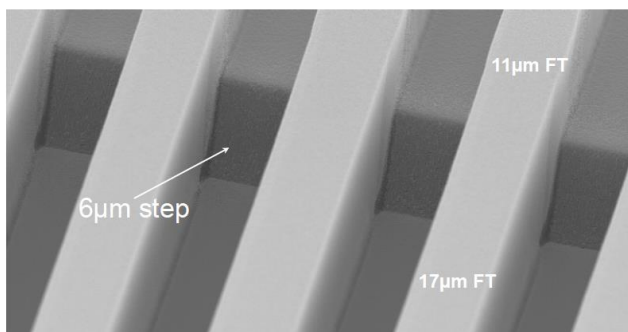


Fig. 6: 5 μm RDL photoresist line/spaces over 6 μm polyimide (PI) step, the photoresist thickness changes from 11 μm to 17 μm

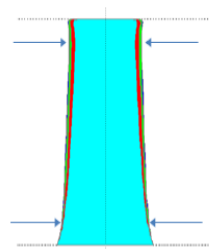


Fig. 7: Modeled linewidth metrology measurement locations

Once the photoresist model is validated, Bossung curves, as shown in Fig. 8 can be generated and sidewall angles, Fig. 9 can be plotted to determine optimal depth of focus and process latitude possible.

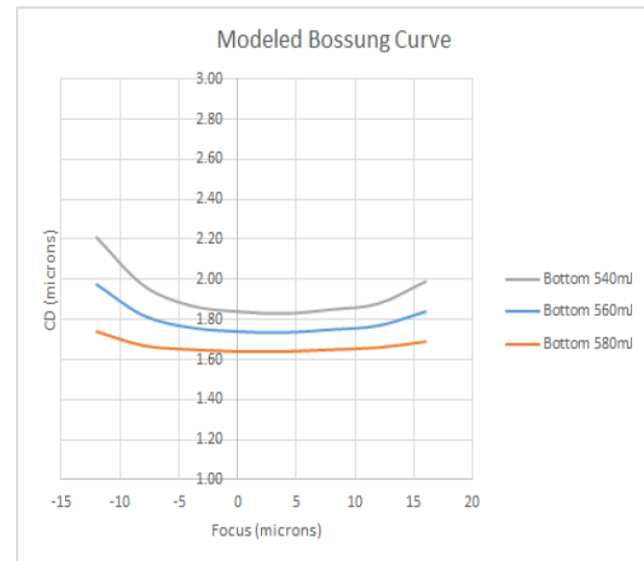


Fig. 8: Modeled Bossung curve

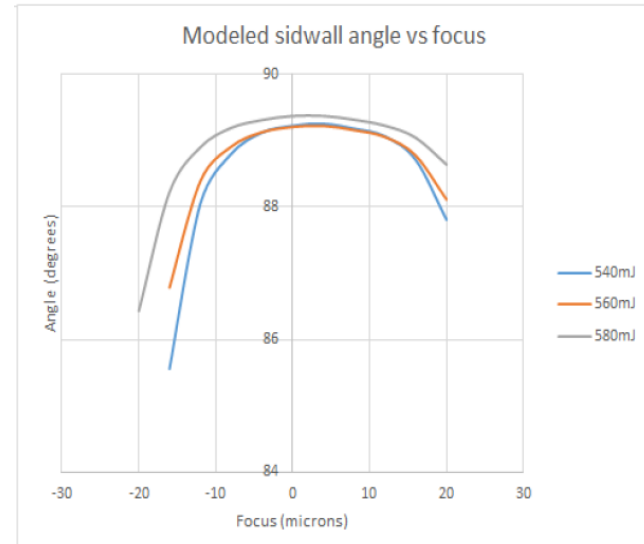


Fig. 9: Modeled sidewall angle through focus

GenISys photoresist software can also be used to create models with negative tone photoresists. Fig. 10 shows the shape of the contrast/gamma curve for AZ15nXT. A model was created based on fitting this curve while varying the development rates, R_{max} and R_{min} , slope and M_{th} parameters.

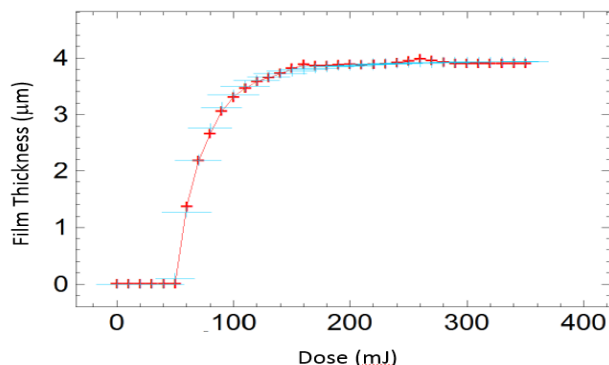


Fig. 10: Gamma curve for AZ15nXT (negative resist)

The 2D photoresist model is based on NA 0.1, sigma 0.7 and i-line wavelength shown in red, and is compared with SEM measured images of 2 μm l/s printed in Fig. 11.

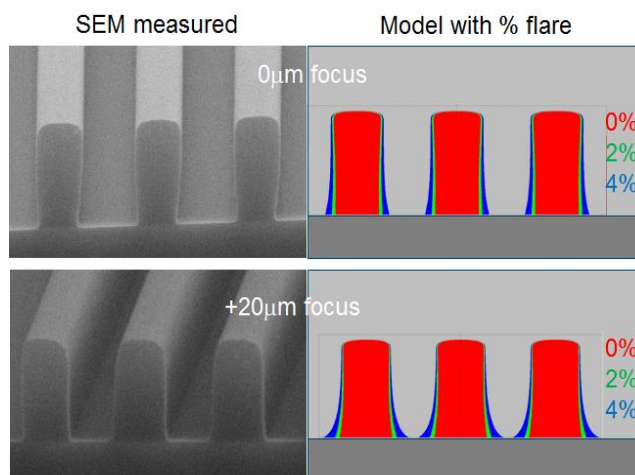


Fig. 11: SEM measured 2 μm l/s vs. 2D photoresist model

The validated model is then used to extrapolate the impact that background intensity or flare has on imagery. Fig. 11 also shows how the dimensions at the bottom of the photoresist are severely affected with increasing amounts of flare. At +20 μm focus and 4% flare the space is not cleared and bridging is observed. Thus, depth of focus is limited as the amount of flare increases. Variation of background intensity or flare can have a significantly detrimental effect on critical dimensions of spaces or vias at the photoresist substrate interface. Printing vias with thick negative photoresists or polyimides can create a foot at the bottom of a contact hole that reduces the useable depth of focus. If the background intensity variation or flare is large enough the hole can be completed scummed over at the bottom. The impact from flare increases with film thickness.

Fig. 12 shows the effect of scumming at the bottom of a 30 μm diameter hole with increasing amounts of flare (%).

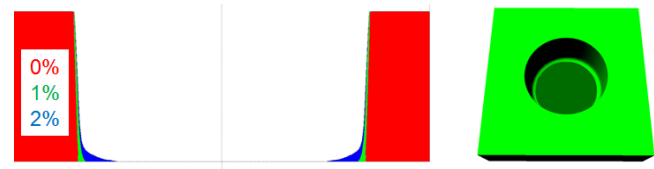


Fig. 12: Model of 15 μm film (negative) exposed at ghi

The variation in background intensity or flare is measured for each exposure tool [3]. A mask is utilized with alternating opaque and transmissive squares. The pattern is projected onto the image plane where a detector mounted in the stage is used for measuring intensity variations under each square over the entire image field. See Fig. 13.

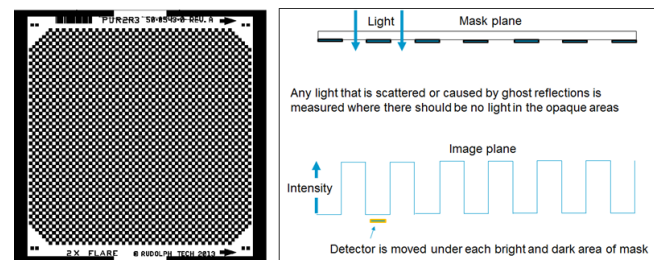


Fig. 13: Flare mask and measurement setup

The variation in background intensity or flare is the % ratio of light intensity projected onto the image plane and is measured in the location of the dark square areas divided by the projected light measured in the bright square areas. Fig. 14A plots the variation in the uniformity from the normalized bright intensity patterns with the 50% transmission opaque reticle and Fig. 14B plots the percent variation from the low intensity patterns divided by the average bright intensity value. In this example the illumination non-uniformity is +/- 2.8%. The total percent flare variation is only 0.3%. The low variation in flare make it ideal for printing vias in thick negative resists and polyimides.

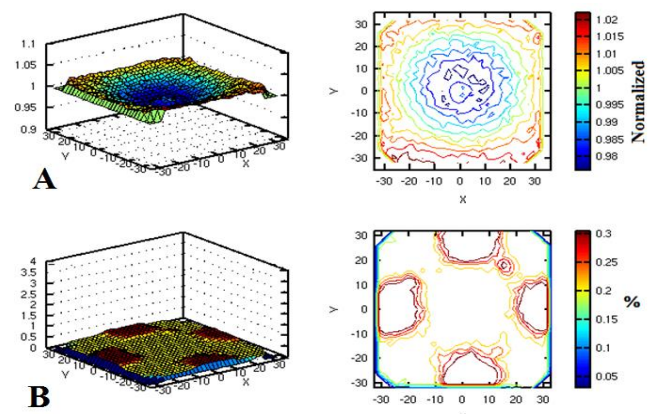


Fig. 14: Example of normalized non-uniformity and flare

Our camera, shown in Fig. 15 with its recently upgraded illumination optics, includes an automated filter wheel for multiple spectral bandwidth options and a high transmission refractive projection optic. Fig. 16 shows the single telecentric lens that is capable of printing twice the field size of the Wynne-Dyson form [4]. The camera has a much larger depth of focus and large magnification adjustment and now can deliver a higher total wattage needed for volume manufacturing [5].

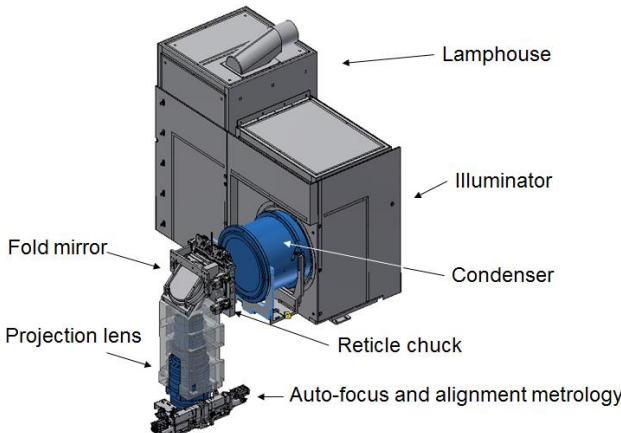


Fig. 15: Step and repeat camera - optical modules

The single telecentric projection lens shown in Fig. 16 provides large magnification adjustment with z-motion of the reticle chuck and re-focus of the camera. The total range of scale and magnification adjust is $\pm 16 \mu\text{m}$ over the $52 \times 66 \text{ mm}$ rectangles or $59.4 \times 59.4 \text{ mm}$ square.

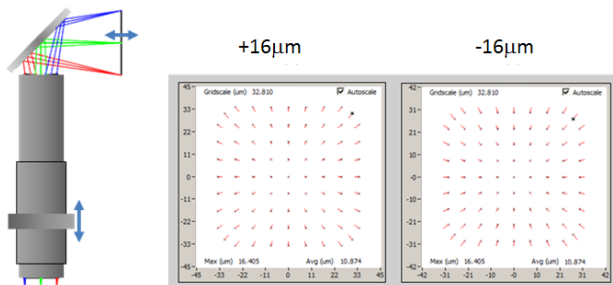


Fig. 16: Single telecentric lens and range of magnification adjustment plotted [6]

Improving overlay over large substrates requires a large range of magnification adjustment. Compensating for overlay errors on dimensionally unstable material and process-induced variation is achieved with a closed loop process to improve yield. Die placement positions are measured. The analysis of the measurements is then fed forward to determine magnification and scale correction to

the stepper before exposures are made. Tool parameters are monitored to control and optimize the process. A compensation method used is diagrammed in Fig. 17.

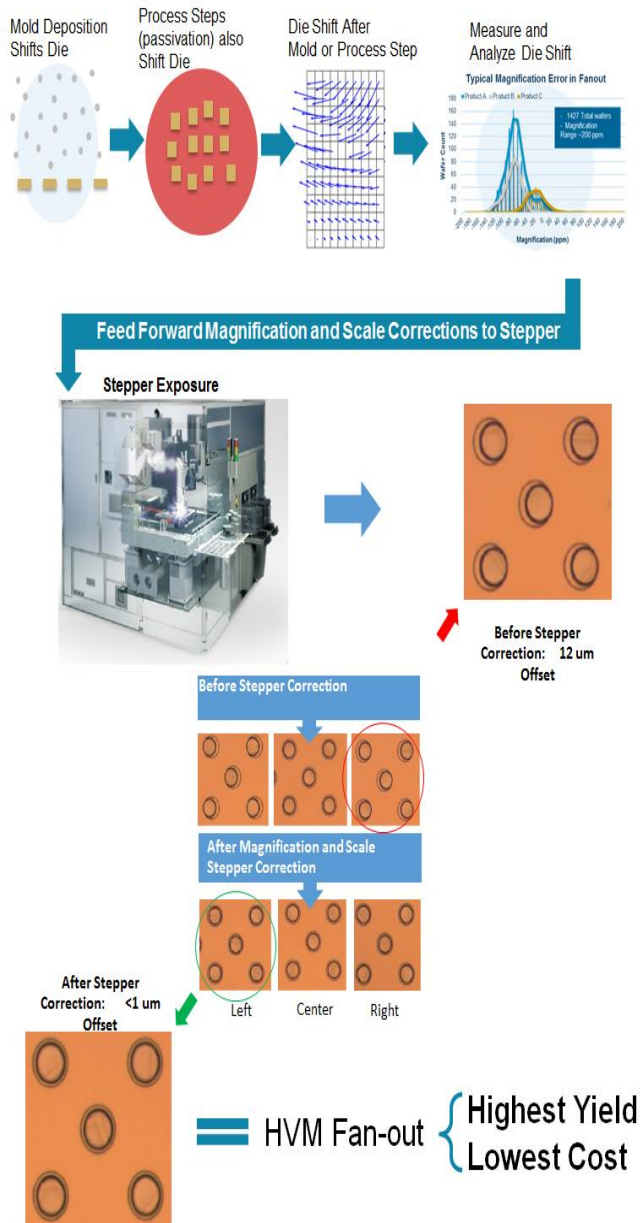


Fig. 17: Fan-out process showing large magnification adjustment

Wafer and panel warpage is common for back-end applications: $>2 \text{ mm}$ up to 6 mm . It is driven by thick films and various materials (metal, mold compound, polymers, photoresists, etc.) and with coefficient of thermal expansion (CTE) mismatching. If material warp is too large for automatic bankers or vacuum, a warp assist mechanism can be deployed. See Fig. 18.

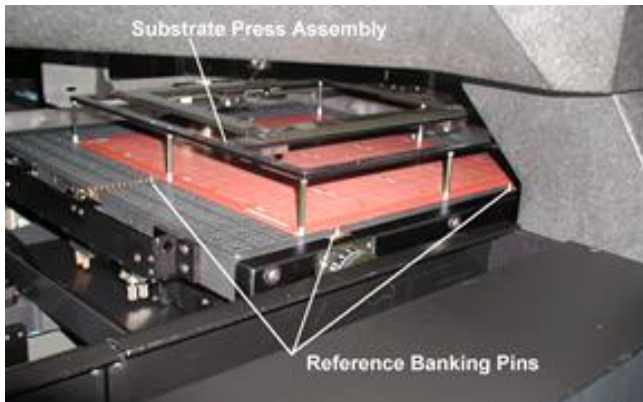


Fig. 18: Stage chuck showing warp assist mechanism

The example in Fig. 19 shows topographical errors of a glass plate vacuumed with the stage chuck. The magnitude of the error is 38 μm . Increased depth of focus with a lower numerical aperture lens along with autofocus at every exposure site enables proper imaging over warped substrates with topographical variations.

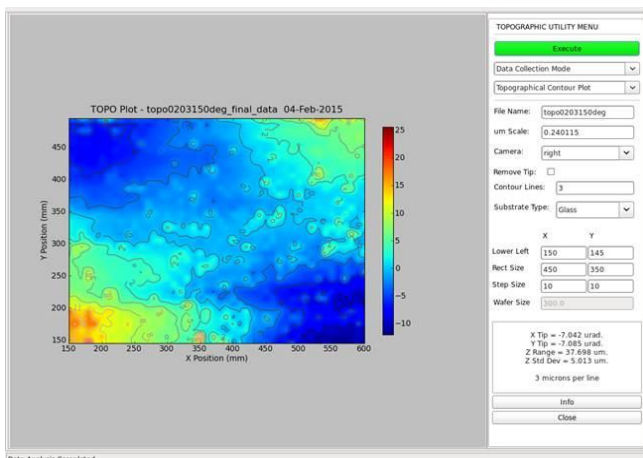


Fig. 19: Topographical map of stage chuck with glass substrate being held in place with vacuum

Fig. 20 shows the method used to minimize the topographic focus errors shown in Fig. 19 using real-time auto-focusing for each exposure.

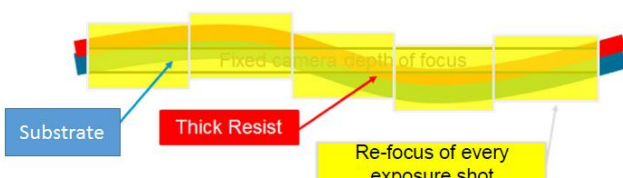


Fig. 20: Auto-focusing at each exposure site with varying topography

Conclusion

Improvements in resist contrast enable low numerical aperture step and repeat cameras to print smaller features with steeper sidewall angles. Resolution in thicker films can be realized over a larger image field with increased depth of focus. This is needed to print on substrates with larger variation in topography. Refocusing in real time for each exposure site minimizes the effects of large substrate topography errors or warpage. Resist modeling aids in determining optimal parameters for increased depth of focus and steeper sidewall angles with varying film thickness. Low background intensity variation or flare in the camera ensures dimensions in negative tone resists and polyimides can be printed in thick films. Overlay errors caused by dimensionally unstable materials or process-induced variables can be greatly reduced over a large exposure field. The single telecentric projection lens with the large scale adjustment for magnification makes it possible to improve overlay over the extended range needed.

ACKNOWLEDGMENT

The authors would like to thank the engineering, application and integration teams at Rudolph Technologies at the Lithography Systems Group (LSG) for their contributions to this paper.

References

- [1] B. Smith, J. Webb, J. S. Peterson, J. Meute, "Aberration evaluation and tolerancing of 193nm lithographic objective lenses," in *Proc. SPIE, Optical Microlithography XI, Volume 3334*, (1998).
- [2] J. Webb, R. McCleary, G. Lopez, Q. Tang, "Comparison of measured and modeled lithographic process capabilities for 2.5D and 3D applications using a step and repeat Camera," in *Proc. IMAPS-47th International Symposium on Microelectronics*, San Diego, CA, 2014.
- [3] J. Kirk, "Scattered light in photolithographic lenses," in *Proc. SPIE, Volume 2197*, p. 566-572 (1994).
- [4] J. Webb, P. Cochet, "Enhanced optical performance for a reduction stepper to meet the challenges for advanced packaging applications" in *Proc. IMAPS- 46th International Symposium on Microelectronics*, Orlando, FL, 2015.
- [5] J. Webb, S. Gardner, E. DaSilveira, "Improved compensation for a reduction stepper to meet the challenges for advanced packaging applications," in *Proc. IMAPS- 46th International Symposium on Microelectronics*, Orlando, FL, 2013.
- [6] Corning Airport GDAT distortion analysis software using National Instruments Corporation license